

Journal of Biomedical Optics

SPIDigitalLibrary.org/jbo

Angular high-speed massively parallel detection spectral-domain optical coherence tomography for speckle reduction

Yuuki Watanabe
Haruyuki Hasegawa
Seiya Maeno

Angular high-speed massively parallel detection spectral-domain optical coherence tomography for speckle reduction

Yuuki Watanabe, Haruyuki Hasegawa, and Seiya Maeno
Yamagata University, Graduate School of Science and Engineering,
4-3-16 Johnan, Yonezawa, Yamagata, 992-8510, Japan

Abstract. We demonstrate speckle reduction based on angular compounding using parallel-detection spectral-domain optical coherence tomography (OCT). An ultrahigh-speed two-dimensional complementary metal-oxide semiconductor camera acquired angular and spectral interference fringes (128×1024 pixels) simultaneously at 15,000 frames/s for a single lateral point. A signal-to-noise ratio improvement of 8 dB was achieved for imaging human skin *in vivo* by averaging 121 angle-resolved OCT images. © 2011 Society of Photo-Optical Instrumentation Engineers (SPIE). [DOI: 10.1117/1.3589093]

Keywords: speckle reduction; optical coherence tomography; angular compounding; ultrahigh-speed 2D CMOS camera.

Paper 11091LR received Mar. 2, 2011; revised manuscript received Apr. 12, 2011; accepted for publication Apr. 15, 2011; published online Jun. 1, 2011.

Optical coherence tomography (OCT) is a noninvasive, non-contact, imaging modality used to obtain cross-sectional images of tissue structures with high resolution. Imaging speed and quality are important in clinical OCT. Fourier-domain OCT has the advantage of improved imaging speed and sensitivity compared with time-domain OCT. However, OCT images of biological tissues contain speckles from multiple scattering within the sample. Speckles appear as a grainy texture in the image and conceal structural details. However speckles provide information about both the structure of the imaged object as well as image noise. Therefore, several approaches have been developed for speckle reduction using angular compounding,¹⁻⁴ frequency compounding,⁵ polarization compounding,⁶ and strain compounding.^{7,8}

Angular compounding is performed by averaging multiple images acquired at different angles. The signal-to-noise ratio (SNR) is improved by taking the square root of the number of averaged images;¹ however, the number of averaged images is too low to reduce speckles, and the compounded images still contain speckle noise.

A wavelength-swept source and an InGaAs line-scan camera with 400 pixels can simultaneously acquire 100 times more angles than previous approaches.⁹ However, the A-line rate is

too slow (25 Hz) for imaging *in vivo* because the limited camera readout rate (~19 kHz) prevents the acquisition of interference signals for adequate depth ranges. To achieve rapid angular compounding, light from different backscattering angles is detected selectively by adding a scanning mirror.¹⁰ However, this beam scanning decreased the imaging speed for a single lateral point. Thus, many angle-resolved OCT images must be acquired simultaneously for speckle reduction with improved SNR without reduced imaging speed.

In this paper, we propose a novel method for speckle reduction based on angular compounding using a parallel-detection spectral-domain (SD)-OCT with an ultrahigh-speed two-dimensional (2D) complementary metal-oxide semiconductor (CMOS) camera (1024×128 pixels, 15,000 frames/s). A 2D camera (1024- and 128-pixel) detected spectral interference fringes and angular components, respectively. An improvement in SNR of 8 dB was achieved for imaging human skin *in vivo* by averaging 121 angle-resolved OCT images.

A schematic of our parallel-detection SD-OCT system is shown in Fig. 1. The collimated output beam of a superluminescent diode (SLD) (QSDM-830-9; QPhotonics) with center wavelength of $\lambda_0 = 838$ nm, and spectral width of $\Delta\lambda = 26$ nm was split into sample and reference arms. Achromatic lenses (diameter = 25 mm, focal length = 35 mm) were inserted into both arms. The measured lateral resolution was 12 μm . The reference mirror was not placed on the focal point, but was positioned by adjusting the achromatic lens in the reference arm to detect angle-resolved interference fringes. Light returning from the two arms was recombined and directed to a diffraction grating (volume phase holographic grating, 1200 lines/mm; Wasatch Photonics) and then focused on a 2D CMOS camera (1024×128 pixels, $17 \times 17 \mu\text{m}^2$ pixel size, 10-bit resolution, 15,000 frames/s, FASTCAM-MAX; Photron) using an achromatic lens ($f = 150$ mm). The horizontal (1024 points) and vertical (128 points) pixels of the 2D camera detected spectral interference fringes and the angular components of the backscattered light from a sample, respectively and the expanded reference beam that was generated by displacement of the achromatic lens in the reference arm. As the probe beam scanned at 29.3 Hz using a sawtooth waveform (95% duty cycle), modified to reduce mechanical vibrations, a spectral data set of 512 A-lines was obtained at intervals of 34.1 ms.

To obtain angle-resolved OCT images, we calculated the reference intensity distribution by averaging 512 captured images to remove the dc components, including the intensity of the reference beam and the fixed pattern noise. Next, the dc removed interference signal (1024 points) was resampled from wavelength (λ)-space to wavenumber ($k = 2\pi/\lambda$)-space by linear interpolation and subsequent application of an inverse Fourier transform. The resampling and Fourier-transform processes were performed for 128 angular points×512 lateral points. The data set of OCT images consisted of 512 A-lines×512 axial pixels with 128 angular points.

In our system, back-reflected light from nonscattering objects was detected at the center of the camera. The backscattered light from scattering media was expanded spatially and detected as angular components in the vertical pixels of the 2D camera. To confirm this difference, we measured a plane mirror as a

Address all correspondence to: Yuuki Watanabe, Yamagata University, Graduate School of Science and Engineering, 4-3-16 Johnan, Yonezawa, Yamagata, 992-8510, Japan. Tel: 81-238-26-3292; Fax: 81-238-26-3292; E-mail: ywata@yz.yamagata-u.ac.jp.

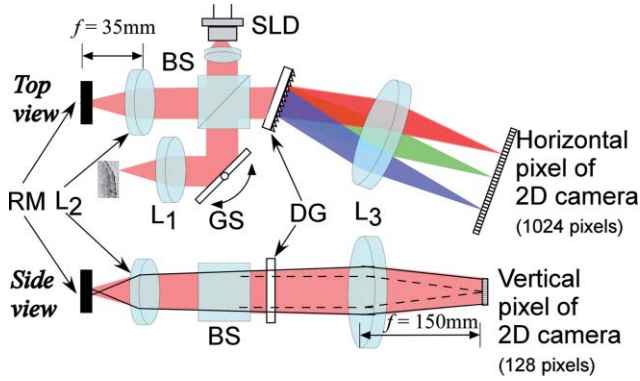


Fig. 1 Schematic of the parallel SD-OCT system with a 2D camera (1024×128 pixels): SLD, superluminescent diode; BS, beam splitter; GS, galvano scanner; DG, diffraction grating; L, achromatic lens; RM, reference mirror. The solid and dashed lines show the reflected beams from the RM and a nonscattering sample, respectively.

nonscattering sample. Figure 2(a) shows an angle- and depth-resolved image (128×512 pixels). The reflected point can be seen only at the center in the angular direction. Figure 2(b) shows the depth profile of a single A-line obtained from Fig. 2(a). For comparison, we measured the depth profile of the same mirror, as shown in Fig. 2(b) when the reference mirror was placed on the focal point of the lens (i.e. conventional SD-OCT setup). With 6.5 mW incident on the sample and 50 dB of sample arm attenuation, the sensitivity of the single-depth profile of our system was 81.8 dB for the peak at 0.25 mm and was smaller than the conventional SD-OCT (88.2 dB). This decrease was caused by the low visibility of interference fringe due to the mismatch between the sample and reference beams. Note that the sensitivity, defined as the minimum detectable reflectance

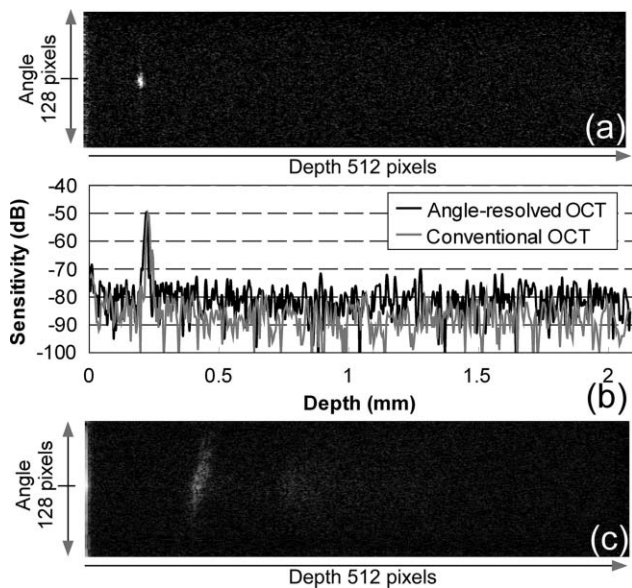


Fig. 2 (a) Angle- and depth-resolved image of a plane mirror (128×512 pixels). (b) Depth profiles at angle-resolved OCT and conventional OCT. (c) Angle- and depth-resolved image of a human fingertip (128×512 pixels).

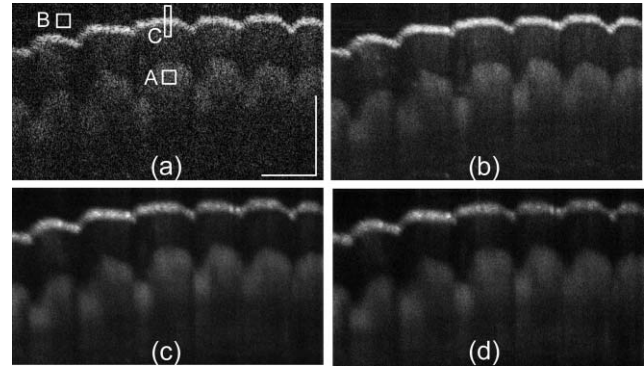


Fig. 3 OCT images of a human fingertip *in vivo* with an imaging range of 2.8×1.1 mm² (lateral × axial) by compounding (a) 1, (b) 11, (c) 51, and (d) 121 angle-resolved images. The scale bar: 0.5 mm.

in the absence of speckles, differed from the SNR improvement due to speckle reduction.

Next, we measured angle-resolved OCT images of a human fingertip *in vivo*. The OCT signals were spatially spread in the angular direction of the angle- and depth-resolved image (128×512 pixels), as shown in Fig. 2(c). We averaged the A-lines by adding them one by one on both sides from the center of the angle- and depth-resolved image. Figures 3(a)–3(d) show OCT images with an imaging range of 2.8×1.1 mm² (lateral × axial) by compounding 1, 11, 51, and 121 angle-resolved OCT images, respectively. The speckle reduction in Figs. 3(b)–3(d) was compared with that of the single angle-resolved OCT image [Fig. 3(a)].

We estimated SNR improvement based on the number of averaged images in angular compounding, as shown in Fig. 4. SNR is defined as the ratio of the mean, $\langle I \rangle$, to the standard deviation of the intensity, σ_I : $SNR = \langle I \rangle / \sigma_I$. We calculated the SNR of the region of interest (ROI) with 20×20 pixels in the speckle-reduced OCT images. The ROI in A and B are the OCT signals and the background of the images, respectively [Fig. 3(a)]. The SNR was improved by increasing the number of averaged images, N_A . The images were averaged incoherently, improving SNR in proportion to the square root of the number of averaged images, $N_A^{1/2}$. In ROI B (background), SNR improvement agreed with $N_A^{1/2}$ because the background noise was random. In ROI A, the improvement curve agreed with $N_A^{1/2}$ until $N_A = 9$ and then deviated gradually from $N_A^{1/2}$. One reason for this difference was the intensity distribution of the backscattered beam and refer-

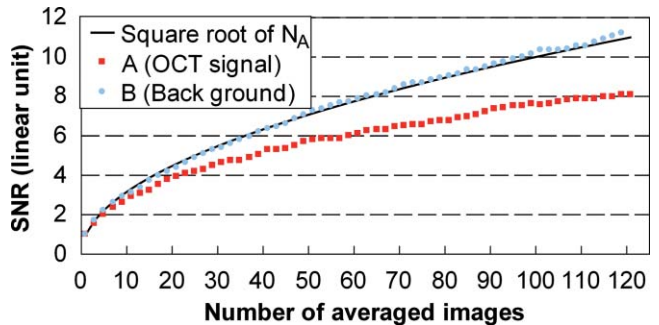


Fig. 4 SNR improvement as a function of the number of averaged images.

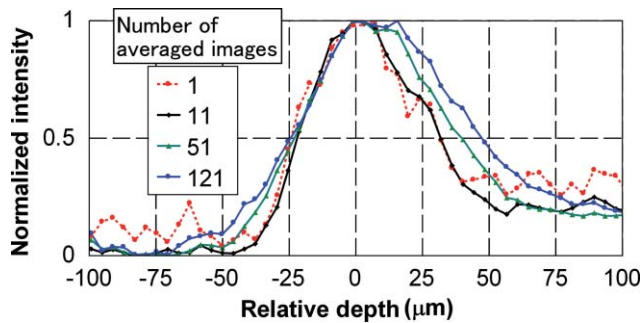


Fig. 5 Depth profiles at surface in Fig. 3.

ence beam, which decreased in the angular direction. The SNR improved by 8 dB at $N_A = 121$, which was 3 dB less than $N_A^{1/2}$. As emphasized by Schmitt¹ the types of speckle are classified as signal-carrying speckle and signal-degrading speckle. The signal-carrying speckle is generated from the sample volume in the focal zone of the imaging optics. The signal-degrading speckle is created by the out-of-focus light that scatters multiple times. To investigate the degrading of axial resolution by multiple scattering events, we obtained the depth profiles that was averaged 10 A-lines at the ROI C in Fig. 3(a), as shown in Fig. 5. The depth profile width at the surface was almost the same at $N_A = 11$. However, it broadened by a factor of ~ 1.4 at $N_A = 121$. Thus, the wide angular components recorded the backscattered angular images as well as some out-of-focus images. Therefore, there is a trade-off between resolution and SNR for wide angular images. If the OCT system utilizes a broadband light source to achieve higher axial resolution (2 to $3\mu\text{m}$), each angle-resolved interference signal needs to compensate the dispersion mismatch using the different parameters because each reference beam has different aberrations in the optical system. The advantage of our proposed method is the acquisition of many angle-resolved OCT images for speckle reduction without reduced imaging speed. However our method works only in a free-space OCT system. To realize our method in a fiber-optic OCT, a fiber bundle may be useful to detect the scattered light as angular components. Fourier domain angle-resolved low coherence interferometer with a fiber bundle probe has been demonstrated for the measurement of depth-resolved angular scattering distributions.¹¹ In future work we will consider its feasibility of speckle reduction in a fiber-optic OCT system.

In conclusion, we demonstrated speckle reduction based on angular compounding using SD-OCT with an ultrahigh-speed 2D CMOS camera. This system used a 2D camera instead of a line-scan camera and the moved lens in the reference arm in conventional free-space SD-OCT systems. The horizontal (1024 points) and vertical (128 points) pixels of the camera detected spectral interference fringes and angular components at 15 kHz, respectively. An improvement in SNR of 8 dB was achieved for imaging human skin *in vivo* by averaging 121 angle-resolved OCT images.

Acknowledgments

This study was partially supported by Industrial Technology Research Grant Program in 2005 from New Energy and Industrial Technology Development Organization of Japan.

References

1. J. M. Schmitt, "Array detection for speckle reduction in optical coherence microscopy," *Phys. Med. Biol.* **42**(7), 1427–1439 (1997).
2. M. Bashkansky and J. Reintjes, "Statistics and reduction of speckle in optical coherence tomography," *Opt. Lett.* **25**(8), 545–547 (2000).
3. N. Iftimia, B. E. Bouma, and G. J. Tearney, "Speckle reduction in optical coherence tomography by 'path length encoded' angular compounding," *J. Biomed. Opt.* **8**(2), 260–263 (2003).
4. H. Wang and A. M. Rollins, "Speckle reduction in optical coherence tomography using angular compounding by B-scan Doppler-shift encoding," *J. Biomed. Opt.* **14**(3) 030512 (2009).
5. M. Kobayashi, H. Hanafusa, K. Takada, and J. Noda, "Polarization-independent interferometric optical-time-domain reflectometer," *J. Lightwave Technol.* **9**(5), 623–628 (1991).
6. M. Pircher, E. Gotzinger, R. Leitgeb, A. F. Fercher, and C. K. Hitzenberger, "Speckle reduction in optical coherence tomography by frequency compounding," *J. Biomed. Opt.* **8**(3), 565–569 (2003).
7. B. F. Kennedy, T. R. Hillman, A. Curatolo, and D. D. Sampson, "Speckle reduction in optical coherence tomography by strain compounding," *Opt. Lett.* **35**(14), 2445–2447 (2010).
8. B. F. Kennedy, A. Curatolo, T. R. Hillman, C. M. Saunders, and D. D. Sampson, "Speckle reduction in optical coherence tomography images using tissue viscoelasticity," *J. Biomed. Opt.* **16**(2), 020506 (2011).
9. A. E. Desjardins, B. J. Vakoc, G. J. Tearney, and B. E. Bouma, "Speckle reduction in OCT using massively-parallel detection and frequency-domain ranging," *Opt. Express* **14**(11), 4736–4745 (2006).
10. A. E. Desjardins, B. J. Vakoc, W. Y. Oh, S. M. Motaghianezam, G. J. Tearney, and B. E. Bouma, "Angle-resolved optical coherence tomography with sequential angular selectivity for speckle reduction," *Opt. Express* **15**(10), 6200–6209 (2007).
11. J. W. Pyhtila, J. D. Boyer, K. J. Chalut, and A. Wax, "Fourier-domain angle-resolved low coherence interferometry through an endoscopic fiber bundle for light-scattering spectroscopy," *Opt. Lett.* **31**(6), 772–774 (2006).